General Disclaimer

One or more of the Following Statements may affect this Document

- This document has been reproduced from the best copy furnished by the organizational source. It is being released in the interest of making available as much information as possible.

- This document may contain data, which exceeds the sheet parameters. It was furnished in this condition by the organizational source and is the best copy available.

- This document may contain tone-on-tone or color graphs, charts and/or pictures, which have been reproduced in black and white.

- This document is paginated as submitted by the original source.

- Portions of this document are not fully legible due to the historical nature of some of the material. However, it is the best reproduction available from the original submission.

NASA CR-170569

M-1829

MINI-CAVITY-DUMPED LASER

Dr. Ed Reed
Sylvania Systems Group
Western Division
GTE Products Corporation
P.O. Box 188
Mountain View, CA 94042

December 1981
Final Report for Period September 1980 - September 1981

Prepared for

GODDARD SPACE FLIGHT CENTER
GREENBELT, MARYLAND 20771

TECHNICAL REPORT STANDARD TITLE PAGE

1. Report No. 1	2. Government Accession No.	3. Recipient's Catalog No.
4. Title and Subtitle Mini-Cavity-Dumped Laser		5. Report Date December 1981 6. Performing Organization Code
7. Author(s) Dr. Ed Reed		8. Performing Organization Report No.
9. Performing Organization Name and Address Sylvania Systems Group Western Division P. O. Box 188 Mountain View, CA 94042		10. Work Unit No. 11. Contract or Grant No. NAS5-26224
12. Sponsoring Agency Name and Address Tom Johnson Goddard Space Flight Center Greenbelt, MD 20771		13. Type of Report and Period Covered Final Report Sept 1980 - Sept 1981 14. Sponsoring Agency Code

15. Supplementary Notes

Presented at the Lasers '81 Conference, New Orleans, LA, December 1981

16. Abstract

Lasers for use in high-precision satellite-ranging systems consist typically of an oscillator followed by several amplifier stages. While the shortest optical pulses are achieved by using a mode-locked oscillator, such an oscillator is incompatible with the compact design needed in future, highly mobile systems. The laser oscillator reported here achieves pulse lengths approaching those obtainable by mode locking, but in a much more compact and stable design. The oscillator uses two $LiNbO_3$ Pockels cells inside the resonator. One Q-switches the oscillator, and the other is used in a pulse-slicing scheme to cavity dump a portion of the circulating optical energy. The length of the optical output pulse was measured to be 425 $\pm$50 picoseconds.

17. Key Words (Selected by Author(s))	18. Distribution Statement
Cavity-dumping Pulse-slice Nd:YAG laser oscillator Short-pulse Satellite ranging	

19. Security Classif. (of this report)	20. Security Classif. (of this page)	21. No. of Pages	22. Price*
Unclassified	Unclassified	47	

*For sale by the Clearinghouse for Federal Scientific and Technical Information, Springfield, Virginia 22151.

SYLVANIA SYSTEMS GROUP-WESTERN DIVISION
GTE PRODUCTS CORPORATION
Post Office Box 188
Mountain View, California 94042

MINI-CAVITY-DUMPED LASER

Contract No. NAS5-26224

December 1981

Prepared By
Dr. Ed Reed

Preface

The objective of the Mini-Cavity-Dumped Laser program has been to demonstrate a Nd:YAG laser oscillator which uses pulse-slice cavity dumping to achieve optical pulses of 250 picoseconds full-width half-maximum. Other major laser performance goals have been that it provide at least 100 microjoules of energy output per pulse, that the mode quality of the output beam be not worse than 24 millimeters-milliradians, and that it operate at pulse repetition frequencies up to 20 Hz.

A breadboard oscillator was assembled and tested. An optical pulsewidth of 425 ±50 picoseconds full-width half-maximum was achieved. The measured pulse energy was 225 ±75 microjoules, the pulse repetition frequency was 20 Hz, and the output beam quality was 12 millimeters-milliradians.

It is recommanded that future work be concentrated in two areas. First, the oscillator's mechanical design should be improved. Second, the electrical switching speed of the pulse-slicer driver/crystal combination should be increased to achieve pulsewidths the order of 250 to 300 picoseconds.

TABLE OF CONTENTS

LIST OF ILLUSTRATIONS

LIST OF TABLES

Section 1

INTRODUCTION AND SUMMARY

Lasers used in high-precision satellite-ranging systems typically consist of an oscillator followed by several amplifier stages. While the shortest optical pulses are obtained by using a modelocked oscillator, such an oscillator is incompatible with the mobile satellite ranging system now being developed at Goddard Space Flight Center (GSFC). The Mini-Cavity-Dumped Laser program has shown that it is feasible to achieve short (425 picoseconds or less) optical pulses in a very compact design (resonator length approximately 12 centimeters).

The objective of the Mini-Cavity-Dumped Laser program has been to demonstrate a Nd:YAG laser oscillator which uses pulse-slice cavity dumping to achieve optical pulses of 250 picoseconds full-width half-maximum (FWHM). The other major laser performance goals have been that it provide at least 100 microjoules of energy output per pulse, that the mode quality of the output beam be not worse than 24 millimeters-milliradians, and that it operate at pulse repetition frequencies (PRF's) up to 20 Hz. The performance achieved with the breadboard laser oscillator is summarized in Table 1-1.

The breadboard oscillator uses a 2-millimeter diameter by 30-millimeter long Nd:YAG laser rod conductively cooled to a copper mounting block. The rod and the convection-cooled flashlamp are located inside a diffuse-reflecting pump cavity. The laser is Q-switched with a $LiNbO_3$ crystal, and a second $LiNbO_3$ crystal is used to perform the pulse-slice cavity dumping. The optical output pulse exits the laser at an intraresonator polarizer. The intraresonator optical circulating energy can be monitored by measuring the leakage through a 0.5 percent-transmitting resonator end mirror.

Breadboard electronics for driving the Q-switch crystal and for triggering the high-speed driver for the pulse-slicing crystal were designed and fabricated. The electronics provided an adjustable trigger delay which allowed the Q-switch to be fired at the optimum time with respect to the flashlamp current pulse (for maximum intraresonator optical circulating power). Adjustable delays were also provided so that the high-speed driver for the pulse-slicing crystal could be fired at any time

Table 1-1. Summary of Breadboard Oscillator Performance Characteristics

	Goal	Measured Value
Optical Pulsewidth	250 ps FWHM	425 ±50 ps FWHM†
Pulse Energy	>100 μ J	225 ±75 μJ††
PRF	20 Hz	1 to 20 Hz
Beam Mode Quality	<24 mm-mrad	approx. 12 mm-mrad
Flashlamp Input Energy	–	1.4 Joules
Pulse Amplitude Jitter	–	±15% short term*

†Difficult to determine precisely because of instrument limitations. See Subsections 4.1 and 4.3.
††See Subsection 4.4.
*Over time periods of 1 minute.

relative to the Q-switch's firing. This allowed the pulse-slicing crystal's firing to be adjusted so that it occurred simultaneously with the peak in the intraresonator optical circulating power.

The high-speed driver for the pulse-slicing crystal was developed by Pulsar, Inc. It uses a charged transmission line and two spark gaps to develop a 2 to 3 kilovolt (adjustable) pulse, with a risetime (10 to 90 percent) of 400 picoseconds, across a matched load of 50 ohms. The risetime is degraded to approximately 700 picoseconds when driving the pulse-slicing crystal.

Section 2 discusses the optical, electrical, and mechanical design of the breadboard laser oscillator. Section 3 discusses the performance of the high-speed spark-gap driver designed by Pulsar. Section 4 presents and discusses the performance results obtained with the breadboard laser oscillator. Section 5 contains the conclusions and recommendations for future work.

Section 2

LASER DESIGN

2.1 PERFORMANCE GOALS

The desired performance characteristics for the pulse-slice cavity-dumped (PSCD) laser oscillator are shown in Table 2-1. In addition, the following characteristics were considered in the design process:

- Maximum laser rod energy extraction
- High energy efficiency
- High stability against resonator optical misalignment
- Uniform beam intensity
- Low cost

Table 2-1. Laser Oscillator Performance Goals

Pulsewidth	250 ps FWHM
Output Energy	>100 μJ/pulse
Beam Quality	24 mm-mrad or better
PRF	20 Hz maximum

2.2 OPTICAL DESIGN

2.2.1 Optical Schematic

Figure 2-1 shows the optical schematic of the PSCD breadboard oscillator. One end mirror is highly reflecting at 1064 nanometers; the other mirror has a small (0.50 percent) transmission to allow monitoring of the intraresonator optical power. One of the $LiNbO_3$ pockels cells (Q-S) is used to Q-switch the laser, which is accomplished by switching its voltage from the quarter-wave value (about 900 volts) to zero at the appropriate time after the firing of the flashlamp. After the intra-

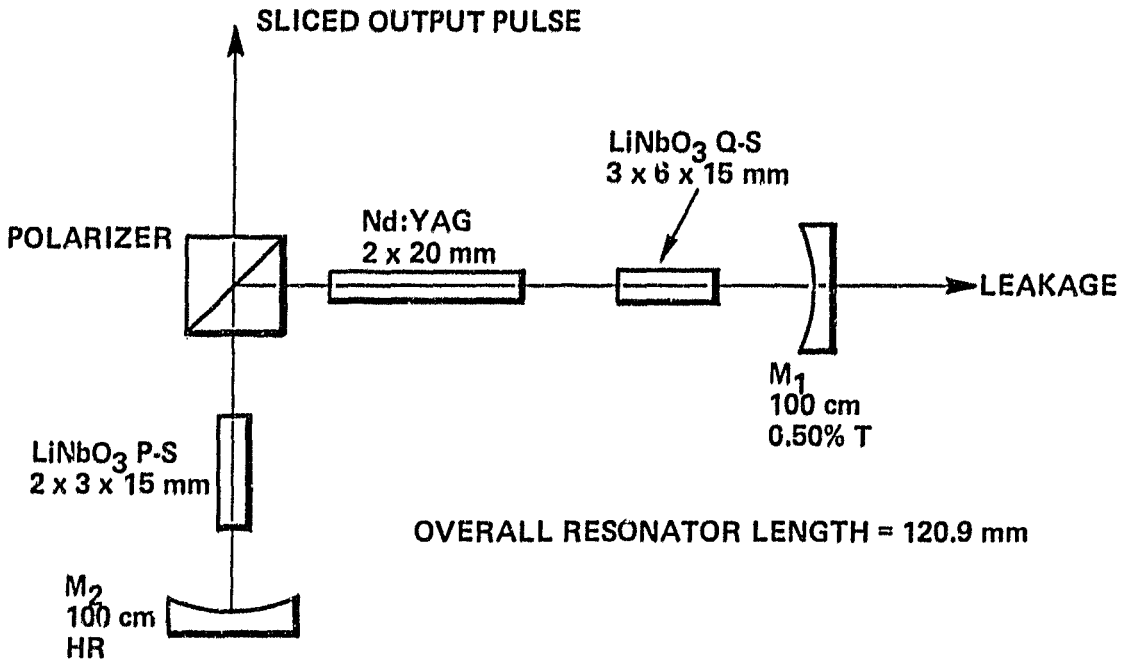

Figure 2-1. Laser Oscillator Optical Schematic

resonator circulating power has reached its maximum, the voltage on the other $LiNbO_3$ (pulse-slicing, or P-S) crystal is switched from zero to its half-wave value. Peak output coupling occurs at the quarter-wave value of this voltage. A half-wave voltage risetime of 500 picoseconds produces an optical pulse length of about 250 picoseconds FWHM.

The electric field in the Q-S crystal is applied along the 3-millimeter direction, and the light propagates along the 15-millimeter direction. The 6-millimeter width was chosen to provide extra surface area if optical damage occurred.

The electric field in the P-S crystal is applied along the 2-millimeter direction. This is discussed more fully in Paragraph 2.3.2.

The laser rod diameter was chosen to be small enough to limit the divergence of the output beam, but large enough to provide the required 100 microjoules of output pulse energy. This is discussed more fully in Paragraphs 2.2.2 and 2.2.3. The resonator design is discussed in Paragraph 2.2.2.

2.2.2 Resonator Design

The resonator configuration affects primarily the divergence of the output beam and the sensitivity of laser operation to a tilt of an end mirror. The diameter of the laser rod can also be considered to be part of the resonator design, because it affects the order of the oscillating mode; this also strongly impacts the laser's energy output. The resonator design steps which were used for the PSCD oscillator are:

a. Keep the resonator as short as practical. This increases laser efficiency. (See Paragraph 2.2.3.)

b. Choose a laser rod diameter which is just large enough to provide the minimum output energy of 100 microjoules per pulse. (See Paragraph 2.2.3.)

c. Choose mirror curvatures small enough that the laser will not be too sensitive to mirror adjustments, but large enough to keep the output beam divergence below 12 milliradians. Flat mirrors provide the lowest beam divergence, but at the expense of extreme adjustment sensitivity.

If θ_{mm} is the full-angle divergence of the multimode beam exiting the resonator, D is the multimode beam diameter, and d is the diameter ($1/e^2$ intensity points) of the oscillating TEM_{00} mode, then

$$D\,\theta_{mm} = \frac{4\lambda}{\pi}\left(\frac{D}{d}\right)^2 , \qquad (2\text{-}1)$$

where λ =1064 nanometers. The TEM_{00} mode size d is given by

$$d = 2\sqrt{\frac{\lambda b}{\pi}}\left[\frac{g_2}{g_1\,(1 - g_1 g_2)}\right]^{1/4} , \qquad (2\text{-}2)$$

where b is the matrix element in the single-pass ray trace matrix, and the g_1, g_2 parameters can be written in terms of the other matrix elements:

$$g_1 = a - \frac{b}{R_1}$$

$$g_2 = d - \frac{b}{R_2} . \qquad (2\text{-}3)$$

R_1 and R_2 are the radii of curvature of the resonator end mirrors.

For the 2-millimeter diameter rod chosen from pulse energy considerations, and the 12-centimeter overall resonator length selected for compactness and energy efficiency (the efficiency is inversely proportional to resonator length), mirror radii of 100 centimeters each were computed to provide a $D\theta_{mm}$ product of about 16 millimeters-milliradians.

2.2.3 Pulse Energy Output

After the Q-switch fires, the optical energy inside the resonator builds up to a maximum, extracting the energy stored in the population inversion of the rod; it then decays because of optical losses. To achieve maximum energy in the sliced output pulse, the peak intraresonator flux must be as high as possible, and the P-S crystal must be operated at the time at which this peak occurs.

Using the theory of Dishington[1] a mathematical expression was derived for the peak value $P_c(max)$ of the one-way intraresonator circulating power P_c:

$$P_c(max) = \frac{c}{2L} \frac{Ah\nu}{k_1\sigma} \frac{\Lambda N_m}{N_t} \left\{ 1 - \frac{N_t}{N_m} \left(1 + \ell n \frac{N_m}{N_t} \right) \right\}, \qquad (2\text{-}4)$$

where

c = speed of light
L = resonator optical length (nd)
A = rod cross-sectional area
k_1 = partition factor (0.4 for Nd:YAG)
σ = stimulated emission cross-section
Λ = single-pass loss coefficient ($e^{-\Lambda}$)
N_m = maximum population inversion per unit volume (upper $^4F_{3/2}$ level only)
N_t = inversion at threshold (depends on Λ)
$h\nu$ = 1.88×10^{-19} joule (for 1064 nm)

Note that N_t, the rod's population inversion per unit volume at threshold, is a function of the loss coefficient Λ; increasing Λ also increases N_t.

An upper limit to the allowed value of circulating power per unit area (P_c/A) is imposed by the damage threshold of $LiNbO_3$: Above 25 to 30 MW/cm^2, damage is likely. Equation (2-4) shows that this maximum value of P_c/A is achieved most efficiently (smallest value of N_m, or flashlamp input energy) when both the resonator length L and single-pass loss coefficient Λ are as small as possible. Using

Equation (2-4), Figure 2-2 was generated. This shows how $P_c(max)/A$ depends on N_m/N_t, for several valuec of loss coefficient Λ. Note, for example, that a one-way optical power density of 30 MW/cm^2 is predicted for a 10 percent single-pass loss when the inversion is about 2.2 times threshold.

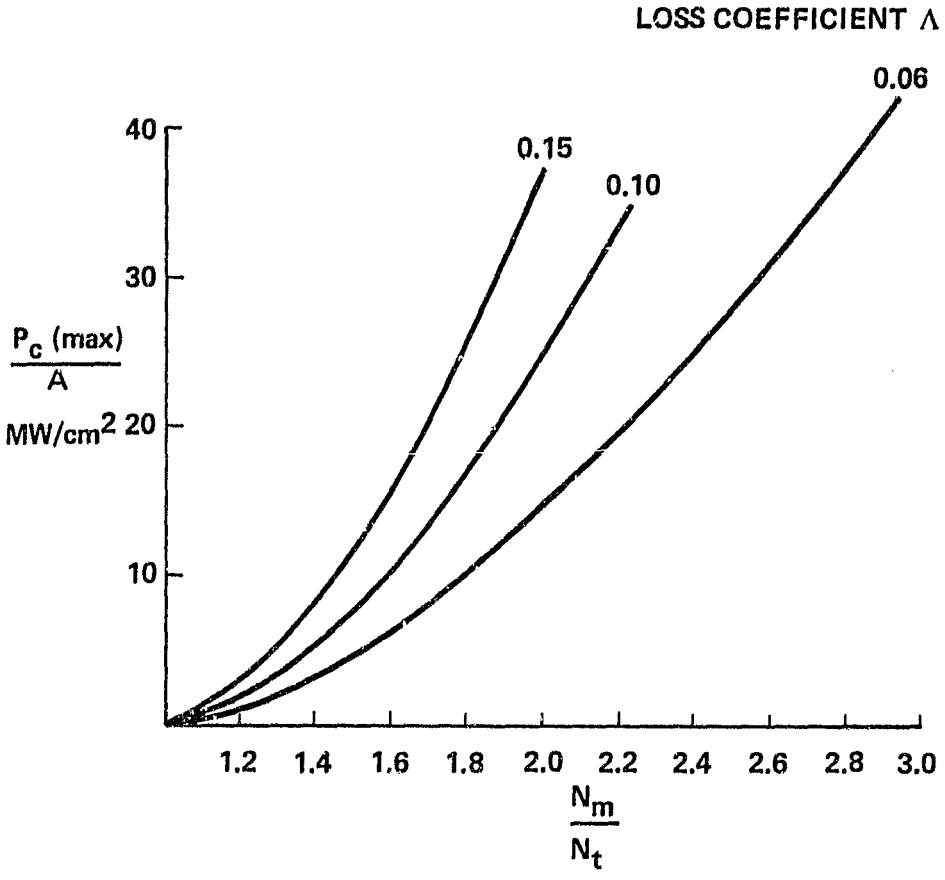

Figure 2-2. Dependence of Peak Circulating Optical Power Density on Pumping Above Threshold

Figure 2-3 shows how much energy is contained in a pulse of 250 picoseconds FWHM sliced from optical beams of various diameters and circulating power densities. The energies were calculated by taking the product (250 picoseconds) x (P_c). This is the same as the integrated energy in a pulse shape described by $\sin^2 \omega t$, which should be the temporal shape of the sliced pulse. (See Paragraph 2.2.5.)

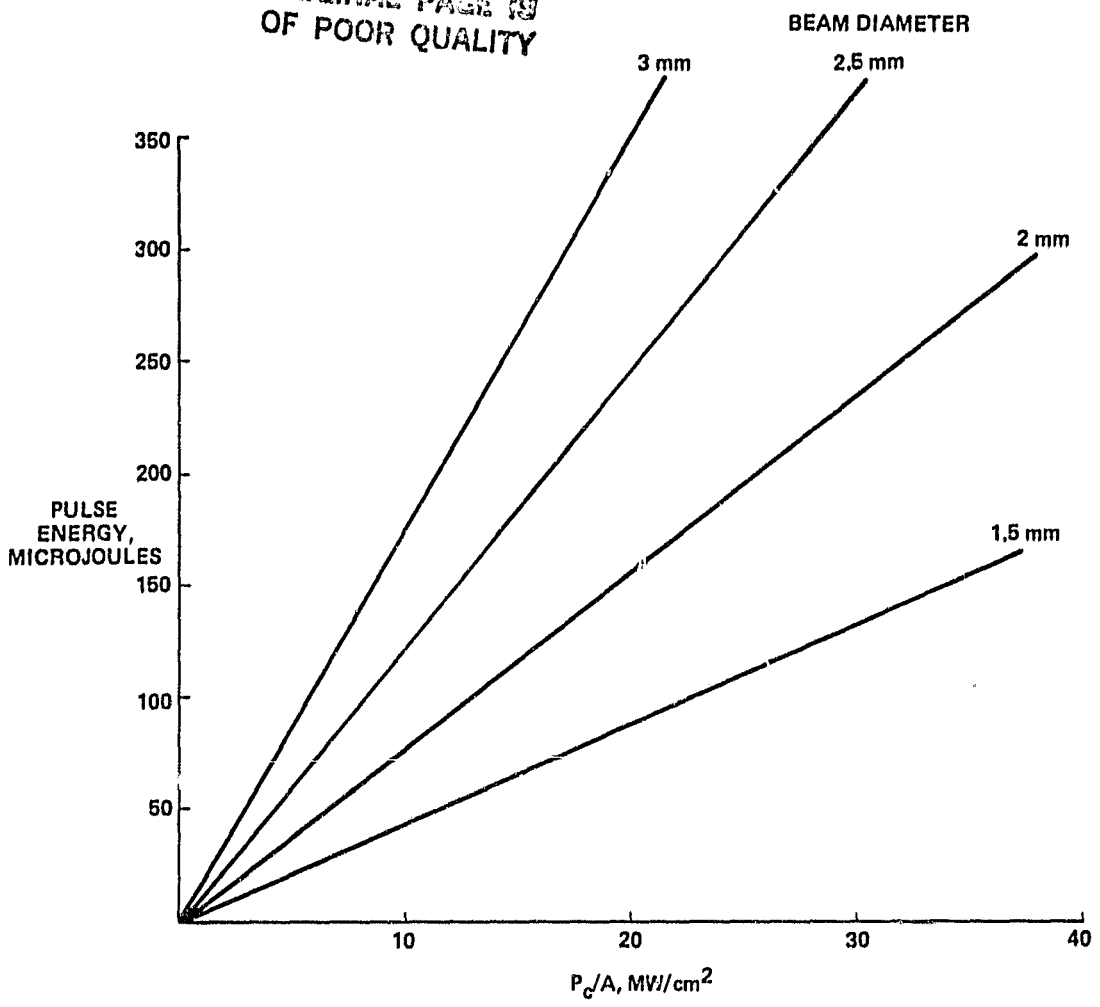

Figure 2-3. Energy Content of a 250-Picosecond P-S Pulse Sliced from Beams of Various Diameters as a Function of Beam Optical Power Density

Besides the sliced output energy, there is another important parameter which depends on N_m and Λ: the buildup time of the Q-switched pulse inside the resonator. For fixed Λ, both $P_c(max)$ and the pulse buildup time will vary from one lamp flash to the next because of small fluctuations in the flashlamp input energy. Figure 2-4 shows this schematically. Since the P-S crystal is fired a fixed time delay after the Q-switch fires, it is important that the fluctuations in the buildup time be kept small compared to the Q-switched pulsewidth. Otherwise, the energy content of the sliced output pulse will fluctuate significantly from pulse to pulse. Fluctuations in the buildup time of around ±5 nanoseconds are acceptable, as this causes an output energy fluctuation of about ±10 percent. (See Section 4.)

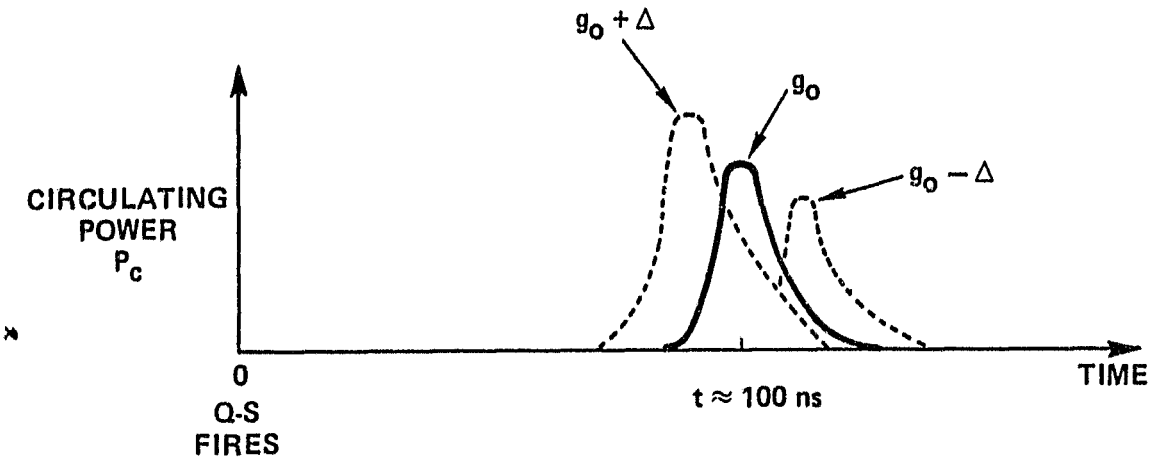

Figure 2-4. Schematic Representation of How the Intraresonator Circulating Power Can Vary from Pulse to Pulse Due to Changes in the Nominal Single-Pass Optical Gain g_o. (The changes Δ result from variations in the flashlamp input energy.)

2.2.4 Flashlamp and Pump Cavity

The breadboard PSCD oscillator was designed to operate with no active cooling of the pump cavity. The lamp is convection and radiation cooled; the rod is cooled by conduction to its copper mounting block. (See Subsection 2.4.) This design was chosen because:

a. It is the simplest pump cavity approach for testing the feasibility of the pulse-slice cavity dumping approach.

b. It was hoped that the design could be carried through to the final engineering design. This would offer distinct advantages over liquid cooling for a mobile laser system.

The size of the flashlamp was chosen to be as small as possible, consistent with cooling constraints. According to the manufacturer, ILC Technology, a quartz-envelope convection-cooled lamp can be operated at a maximum inside wall power loading of 15 W/cm^2. For titanium-doped quartz, chosen because it blocks UV radiation and reduces both laser rod solarization and undue heating, the figure is probably around 12 W/cm^2. Because the expected lamp input energy was around 1 joule

per pulse, approximately 20 watts of flashlamp input power was expected. This led to the choice of a 3-millimeter bore lamp with a 2-centimeter arc length. A krypton gas fill was specified because of the relatively low lamp current densities to be used. The gas pressure was specified to be 700 Torr, a standard value for krypton.

The pump cavity was designed so that the flashlamp and rod are located as close together as possible, and to be easily fabricated. It is a rectangular-shaped cavity, coated with Eastman white reflectance paint, an excellent diffuse-reflecting material. Details of the pump cavity design are contained in Subsection 2.4.

2.2.5 Theoretical Optical Pulsewidth

If a DC voltage V is applied to the P-S pockels cell, the crystal's electro-optic effect will couple a fraction T of the circulating power out of the resonator, where

$$T = \sin^2 \left(\pi \frac{V}{V_{1/2}} \right) . \qquad (2\text{-}5)$$

$V_{1/2}$ is the half-wave voltage value of the crystal at 1064 nanometers. Equation (2-5) applies to an optical round-trip through the crystal.

Equation (2-5) applies to the PSCD oscillator, except that now V is changing very rapidly in time, and varies during the double-pass transit time of the optical beam in the crystal. The round-trip optical transit time in the chosen crystal (15 millimeters long) is about 225 picoseconds. (The resonator mirror adjacent to the P-S crystal is taken to be close enough that the transit time between the two is negligible. This is valid for the breadboard PSCD oscillator.) Under these conditions, one must consider the more general relationship for the output coupling fraction:

$$T = \sin^2 \frac{\Gamma}{2} . \qquad (2\text{-}6)$$

Here Γ is the phase retardation between the ordinary and extraordinary light polarizations, and can be computed from

$$\Gamma = \frac{\pi}{V_{1/2}\, \ell} \int V(t)\, dx , \qquad (2\text{-}7)$$

where x is the distance in the crystal along the optical propagation direction, and ℓ is the crystal's length. The integral is taken over a round-trip in the crystal. Γ must be computed for each point in the beam traversing the P-S crystal.

The integral in Equation (2-7) was graphically computed for the 15-millimeter-long $LiNbO_3$ crystal used in the breadboard PSCD oscillator, assuming V(t) to be a linear ramp which requires 500 picoseconds to reach $V_{1/2}$ (see inset in Figure 2-5). Figure 2-5 shows the computed output pulse shape. If there were no optical transit time effects, the optical output would occur only within a 500-picosecond "window", and the FWHM pulsewidth would be 250 picoseconds. Figure 2-5 shows that the FWHM pulsewidth is still 250 picoseconds, but that there now is a small amount of output coupling outside the 500-picosecond "window" (i.e., the coupling does not go to zero at ±250 picoseconds in Figure 2-5). For comparison, Figure 2-6 shows the output pulse shape for a 30-millimeter long P-S crystal, assuming the same 500 picosecond voltage wareform; the pulsewidth is 280 picoseconds FWHM.

2.3 ELECTRICAL DESIGN

2.3.1 High-Speed Driver Selection

To achieve 250-picosecond optical pulses from the breadboard oscillator, the voltage waveform shown in Figure 2-7 is desired. The full risetime (0 to 100 percent) must be < 500 picoseconds. The voltage must remain high for several 10's of nanoseconds, until the intraresonator optical flux dissipates; otherwise double output pulses will occur. The half-wave voltage $V_{1/2}$ shown in the figure is the transient half-wave voltage, which was found during the course of the laser experiments to be approximately twice the DC half-wave voltage. The transient $V_{1/2}$ for the 2-millimeter high $LiNbO_3$ pulse slicer crystal was found to be approximately 2100 volts. The measured DC half-wave voltage is about 1100 volts.

Five candidate approaches were considered for driving the P-S crystal. Table 2-2 is the trade table which was used to help select an approach to be tested. Both the jitter and the electrical time delay should be within the indicated limits so that the firing of the P-S crystal can be synchronized with the peak in the intraresonator optical flux. The candidates are ranked with 1 being the most attractive approach. The purchase of the spark-gap driver from Pulsar, Inc. was chosen because of their experience in developing similar hardware. The planar triode amplifier approach was a main contender for a while, but was finally ranked low because the vendor (Pico Second Enterprises) had yet to demonstrate a switching

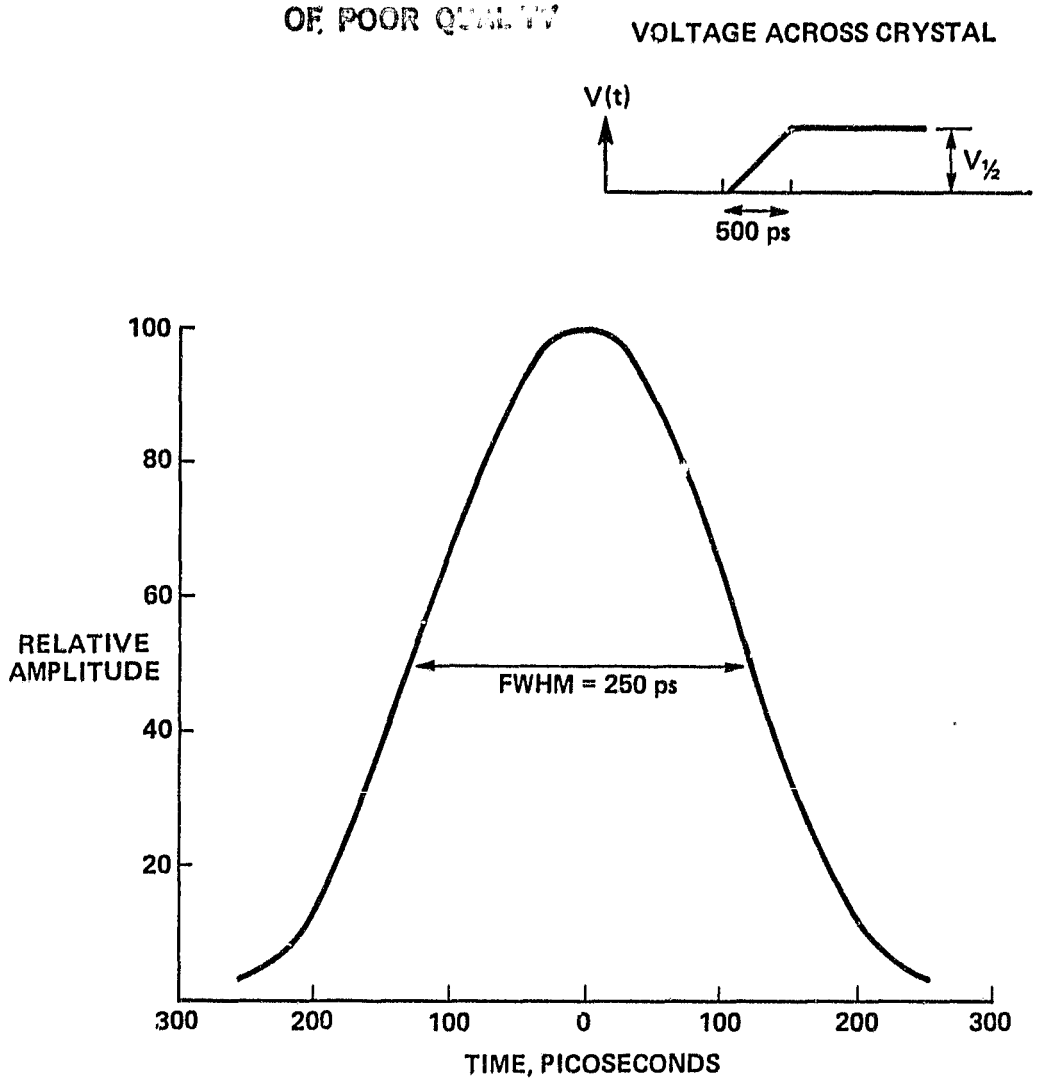

Figure 2-5. Calculated Optical Output Pulse Shape for the 15-Millimeter Long $LiNbO_3$ P-S Crystal for the 500-Picosecond Ramp Voltage Shown.

time of 500 picoseconds, and because its large size made it incompatible with the concept of a miniature laser system. The optically-regenerative silicon switch, ranked 5, is a new idea which originated with Hal Sweeney at GTE. It was not a serious candidate because it has yet to be reduced to practice. It was included in the table for completeness because it had been discussed along with the other candidates. It is an attractive candidate for future systems.

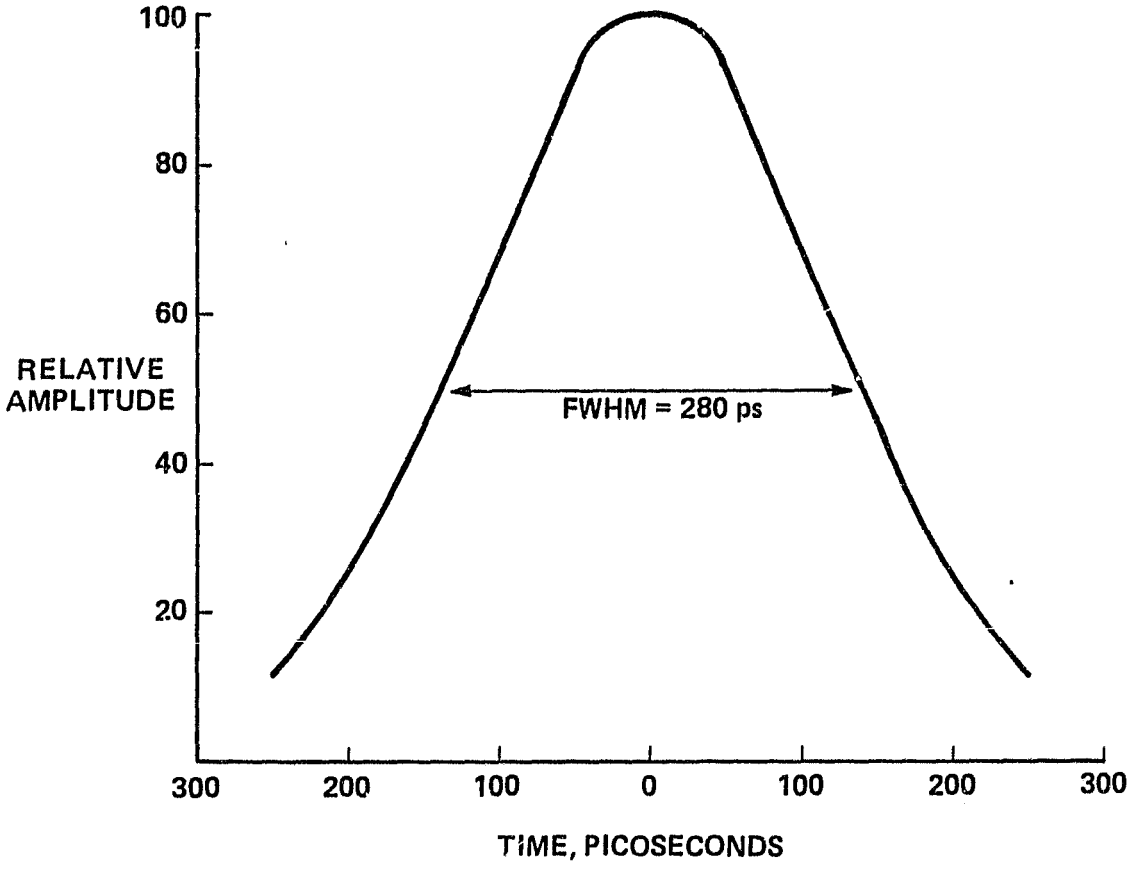

Figure 2-5. Calculated Optical Output Pulse Shape for a 30-Millimeter Long $LiNbO_3$ P-S Crystal. (Applied voltage is the same as in Figure 2-5.)

Figure 2-8 shows a simplified schematic diagram of the spark-gap driver developed by Pulsar, Inc. A 30-foot-long delay line (RG-174 cable) is charged to a variable DC level, up to 6 kilovolts. This charged line is discharged into a second line using a triggered spark-gap. The risetime of the resulting pulse is further reduced by passing it through a second, nontriggered spark-gap before it appears on the output cable. All cables are of 50-ohm impedance. The performance of the driver is discussed in Section 3.

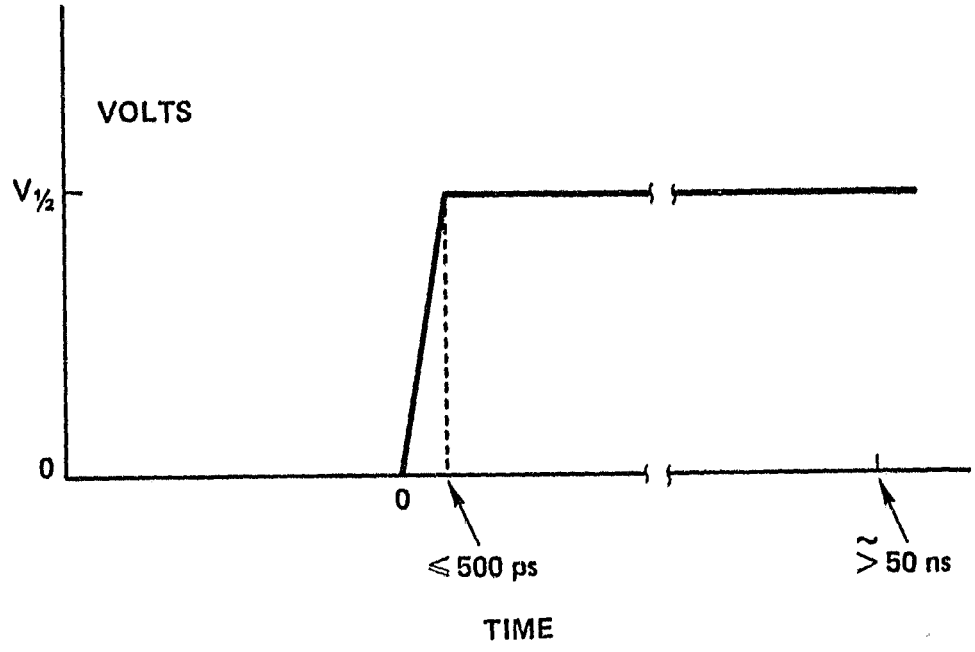

Figure 2-7. Voltage Waveform Desired Across the Pulse-Slicing Crystal

Table 2-2. Trade Table for High-Speed Driver for P-S Crystal

Candidate Approach	Switching Time (0.5 ns required)	Jitter (±3 ns max) (±1 preferred)	Delay (~40 ns max)	Repetition Rate (20 Hz)	Size (Small)	Make/Buy	Cost	Rank
1. Planar Triodes	0.5 ns	±100 ps	15 - 20 ns	>20 Hz	Large	Buy	$12.5K (PSE) + HV supply	4
2. Spark gap	0.5 ns	<± 2 ns	15 - 25 ns	>20 Hz	Small	Buy (Pulsar)	$10.2K (Pulsar) incl. HV supply	1
3. Krytron	~1 ns (½ ns reported)	~± 2 ns	10 - 30 ns	>20 Hz	Small	Buy EGG or build	$795 (EG&G) + development	3
4. Krytron and peaking gap	0.5 ns	± few ns	15 - 35 ns	>20 Hz	Small	Develop	$100 + development	2
5. Optically - Regenerative Silicon Switch	~200 ps Calculated	~none	~none	>20 Hz	Small	Develop	—	5

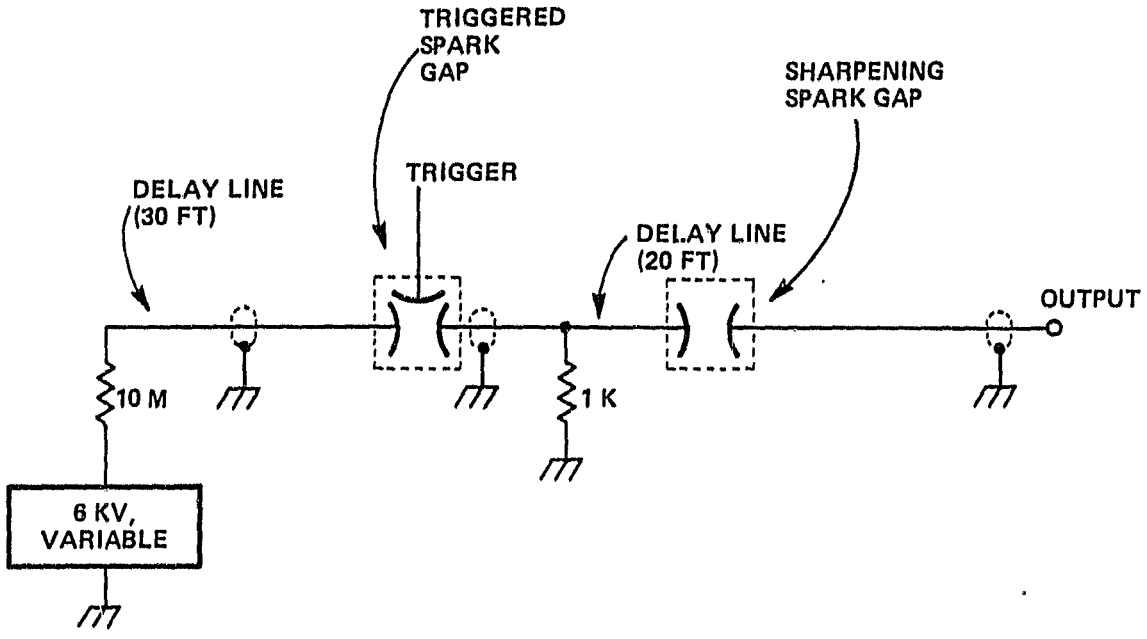

Figure 2-8. Simplified Schematic of the Pulsar Spark-Gap Driver for the Pulse-Slicer Crystal.

2.3.2 Driver/P-S Crystal Interface

The Pulsar spark-gap driver delivers its fast-risetime voltage step on a 50-ohm coaxial cable. When the cable is terminated with any load other than a purely resistive 50-ohms, the risetime of the voltage will be degraded. The goal of the interface design is to mount the P-S crystal, and electrically attach it to the cable in such a way that the voltage risetime degradation is kept to a minimum.

The P-S $LiNbO_3$ crystal is of dimensions 2 x 3 x 15 millimeters, and the electric field is applied along the 2-millimeter direction. Depending on how the crystal is to be electrically connected to the 50-ohm line, it can be viewed as either a lumped or a distributed element. As a lumped element it acts as a capacitance of approximately 9 picofarads. This was computed using the high frequency dielectric constant of $LiNbO_3$, which is 44[2]. (A crystal of dimensions 3x3x15 millimeters, with a capacitance of 6 picofarads, was assumed during the laser design phase. The thickness had to be reduced to 2 millimeters during the testing phase, so that the

required optical retardation could be achieved.) As a distributed element it can be viewed as a transmission line of either 6 or 19 ohms characteristic impedance, depending on the propagation direction of the electrical signal: the larger impedance value applies to electrical propagation along the 15-millimeter crystal length; the smaller value applies to propagation along the 3-millimeter width.

Ideally, the $LiNbO_3$ crystal should be treated as a distributed element, and impedance-matched to the 50-ohm coaxial line of the high-speed driver. In practice, this is not possible using the Pulsar high-speed driver. First of all, the propagation time of the electric field along the 15-millimeter length is

$$\frac{(1.5\ \text{cm})\sqrt{44}}{c} = 332\ \text{picoseconds}, \tag{2-8}$$

which is a large fraction of the voltage risetime, and about three times the optical propagation time. Propagating the voltage along the crystal length would significantly slow down the optical switching time of the crystal. The crystal should thus be electrically fed from the side, so that the electrical propagation distance is the 3-millimeter crystal width. However, as noted above, when driving the pulse-slicer crystal from the side as a distributed element it has a 6-ohm characteristic impedance. Impedance matching from the 50-ohm cable to the crystal would require the Pulsar to deliver a voltage pulse of amplitude V_p, where

$$\frac{V_p^2}{50} = \frac{(2100)^2}{6} \tag{2-9}$$

$$V_p = 6100\ \text{volts}.$$

2100 volts is the switching voltage required on the crystal. The Pulsar unit has a maximum output voltage capability of 3000 volts, about one-half of that required for impedance matching to the $LiNbO_3$ P-S crystal.

The $LiNbO_3$ pulse slicer has thus been treated as a lumped circuit element in electrically mating it with the Pulsar 50-ohm cable. Figure 2-9 shows schematically the two electrical configurations which were considered. The configuration in (a) of the figure preserves the driver output voltage amplitude at the crystal. Also, the effective impedance driving the crystal in (a) is 25 ohms. By comparison, with configuration (b) the voltage at the crystal is doubled due to the pulse reflection

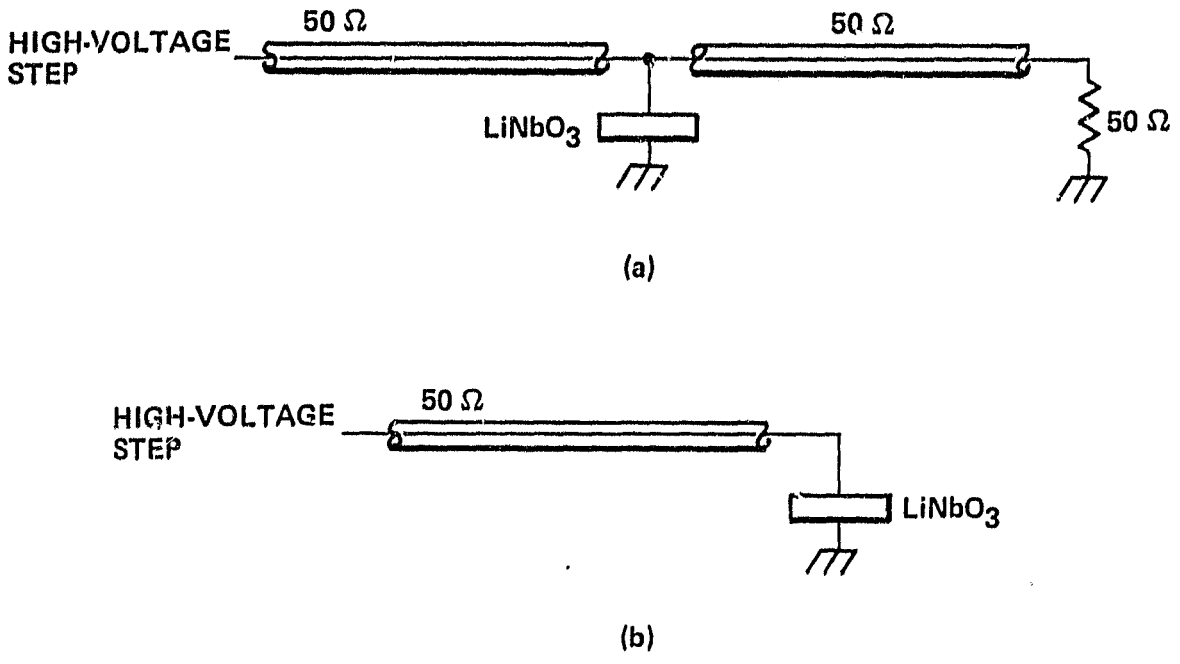

Figure 2-9. Two Possible Methods of Connecting the Slicer Crystal to the 50-ohm Line from the Pulsar High-Speed Driver.

there, and the driving impedance is 50 ohms. Configuration (a) was chosen for use with the breadboard oscillator because of its lower effective driver impedance. This leads to a smaller RC time constant for the cable-crystal combination, which reduces the voltage risetime degradation caused by the crystal's capacitance.

Figure 2-10 shows how the pulse-slicer crystal is mounted and how the electrical drive cables are attached. The two small 50-ohm cables (RG-174) are brought in on one side of the $LiNbO_3$ crystal, and electrical connection to the crystal is accomplished with copper sheets. All dimensions were kept as small as practical to reduce both stray capacitance and propagation times. A Tektronix Time Domain Reflectometer (TDR) was used to configure the electrical connections so as to minimize the risetime degradation caused by the crystal and mount capacitance. The performance of the interface is discussed in Section 3.

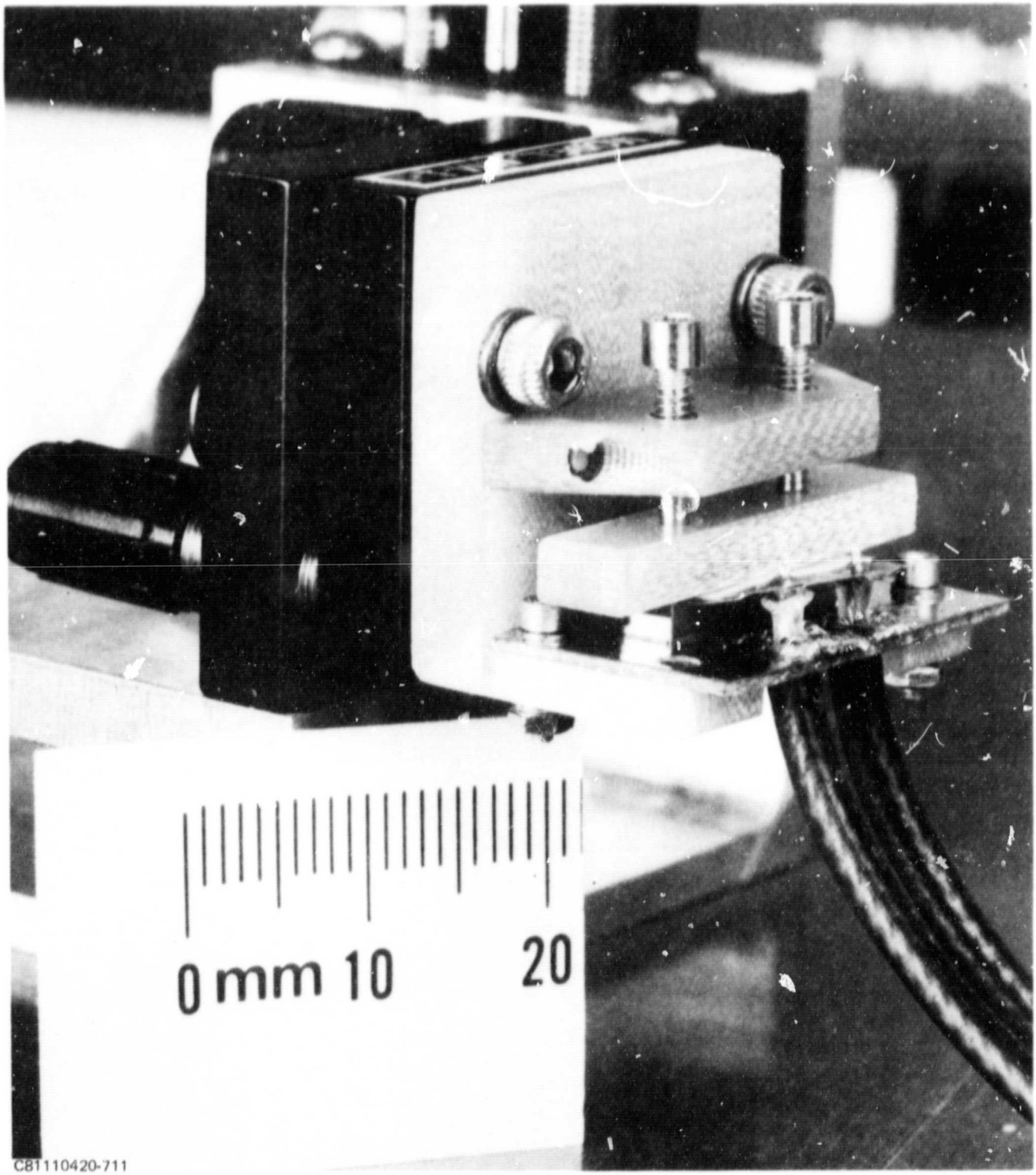

Figure 2-10. Pulse-Slicer Crystal Mount and Cable Interface

2.3.3 Laser Electronics

The Pulsar spark-gap high-speed driver for the P-S crystal was described in Paragraph 2.3.1. The input energy for the flashlamp was obtained from an existing laboratory power supply. The rest of the electronics needed to operate the breadboard laser oscillator were designed and breadboarded during the program. Their design will now be described.

Given the lamp-firing pulse, which controls the discharging of the pulse forming network (PFN) capacitor into the flashlamp, two voltage waveforms need to be generated: a properly timed waveform to operate the Q-switch, and a delayed pulse to trigger the Pulsar high-speed driver. Although not absolutely necessary for laser operation, it might improve performance if the laser's optical gain were electronically stabilized to prevent the fluctuations in the buildup time of the Q-switched pulse, as discussed in Paragraph 2.2.3. Electronics were designed and breadboarded which generated these two waveforms, and which also stabilized the laser's gain. A block diagram of these electronics is shown in Figure 2-11. Laser operation can occur either with or without the electronic gain stabilization, depending on the position of the switch S.

With S in the upper position shown in Figure 2-11, gain stabilization is not occurring. The Enable Pulse Generator produces a 30-microsecond wide pulse whose leading edge can be chosen to occur at a variable time delay (up to 100 microseconds) after receipt of the lamp firing pulse. In operation, the leading edge of this pulse is adjusted to occur toward the end of the flashlamp current cycle, when the population inversion in the laser rod is a maximum. This leading edge controls two trigger pulse generators. The P-S Switch Trigger Generator delivers a fast risetime (a few nanoseconds) pulse to the trigger input connector on the Pulsar high-speed driver. The Q-S Trigger Generator delivers a trigger pulse to the Q-switch driver circuit, which fires the Q-switch. The pulses from each of these two trigger generators can be delayed (independently) from 0.2 to 1.2 microseconds. These two delays are adjusted with respect to each other so that the P-S crystal receives its switching voltage at the time that the intraresonator optical circulating power has reached a maximum. The delay through the Q-switch trigger generator is too small to significantly affect the optimum timing of the Q-switch firing, which has been set by adjusting the delay in the Enable Pulse Generator.

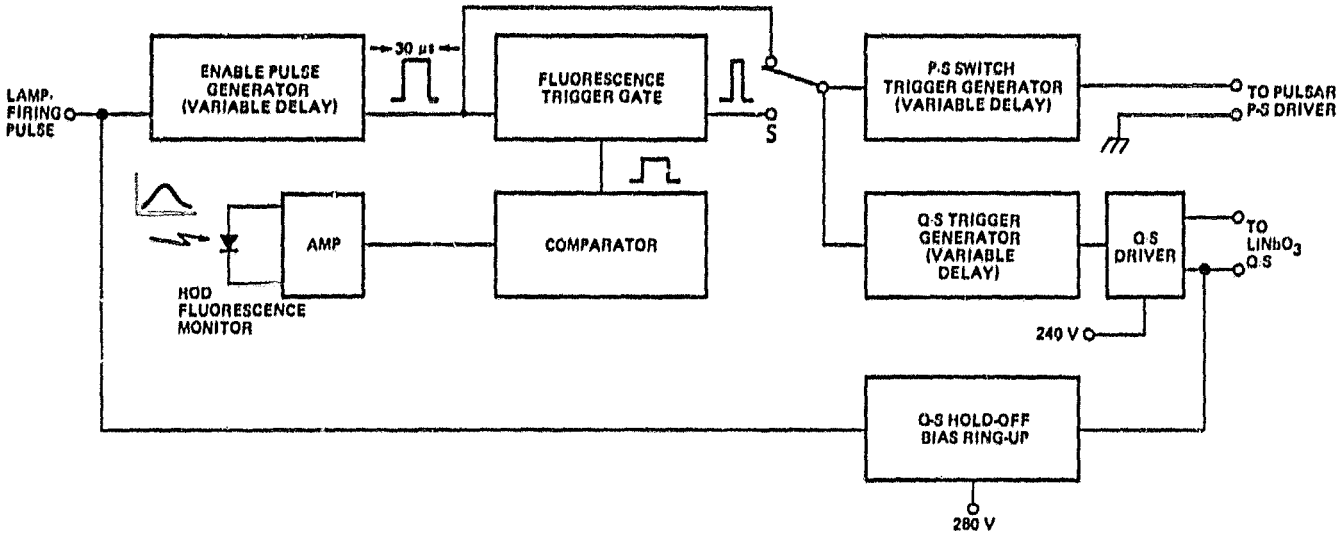

Figure 2-11. Block Diagram of the Timing and Trigger Electronics Designed for the Breadboard Laser Oscillator

Note in Figure 2-11 that the DC holdoff bias (about 850 volts) for the Q-switch is derived from a 280-volt source using a ring-up circuit. This is close to the 240-volt source required for the Q-switch driver. The ring-up circuit was used to demonstrate that a common source of around 300 volts could be used in a final design to supply these two voltages.

Consider now the case when the electronic gain stabilization is being used; the switch S is in the lower position in Figure 2-11. An optical fiber, which can be inserted in the pump cavity top and butts up against the laser rod, delivers rod fluorescence light to a photodiode on the electronics board. A 1064-nanometer band-pass optical filter inserted between the fiber end and photodiode rejects most of the flashlamp light and passes the rod fluorescence. The fluorescence signal is amplified and, when it is above a predetermined level set in the comparator, a voltage is applied to the Fluorescence Trigger Gate. It is desired to trigger the laser Q-switch on the falling edge of the comparator's output voltage; triggering on the leading edge might lead to postlasing, since more laser pumping occurs after buildup

and decay of the Q-switch pulse in this case. Falling-edge triggering is ensured by adjusting the arrival time at the fluorescence trigger gate of the 30-microsecond pulse from the Enable Pulse Generator so that it brackets the arrival time of the falling edge. In addition to guaranteeing falling-edge triggering, the 30-microsecond gating pulse also helps prevent Q-switch triggering due to spurious radiation which might reach the photodiode detector. Because of the priorities on the program, the gain stabilizer was not fully tested; all laser data to be reported (see Section 4) were acquired without gain stabilization.

2.3.4 Pulse Forming Network

An existing flashlamp power supply was used to operate the lamp in the breadboard laser tests. The supply also delivered a lamp-starting pulse and 30 milliamperes of lamp-simmer current. The PFN used an SCR to switch the charged PFN capacitor across the flashlamp. In the circuit used, the polarity reversal of the capacitor voltage, after discharge, is used to close the SCR and allow capacitor recharge. Insufficient voltage reversal can cause the flashlamp to operate continuously, which can destroy it.

The design considerations for the PFN were that it provide a reasonably short current pulsewidth (around 100 microseconds, or less), and that it provide adequate capacitor voltage reversal over the range of lamp input energies used in the tests. This range was from about 0.4 joule to 1.4 joules. The 54 microhenry inductor and 25 microfarad capacitor of the PFN were chosen using the theory of Markiewicz and Emmett[4]. This results in a current pulsewidth of 110 microseconds (the so-called 3T width, where $T = \sqrt{LC}$), and an α value of 0.5 at a lamp input energy of 0.4 joule. (α is a measure of the voltage reversal.) Whenever a lamp input energy value is given in discussing the laser tests, it means the energy actually dissipated in the lamp. It is measured by taking the difference of two PFN capacitor stored energies, that just before lamp firing and that immediately after.

2.4 MECHANICAL DESIGN

Figures 2-12 and 2-13 show the breadboard laser oscillator. The optical components are all mounted on an aluminum baseplate. The Q-switch and pulse-slicing $LiNbO_3$ crystals are each held using commercial mirror mounts and translation stages to facilitate their optical alignment. The resonator mirror mounts are commercial (Oriel), and are mounted to the baseplate with gusseted fixtures.

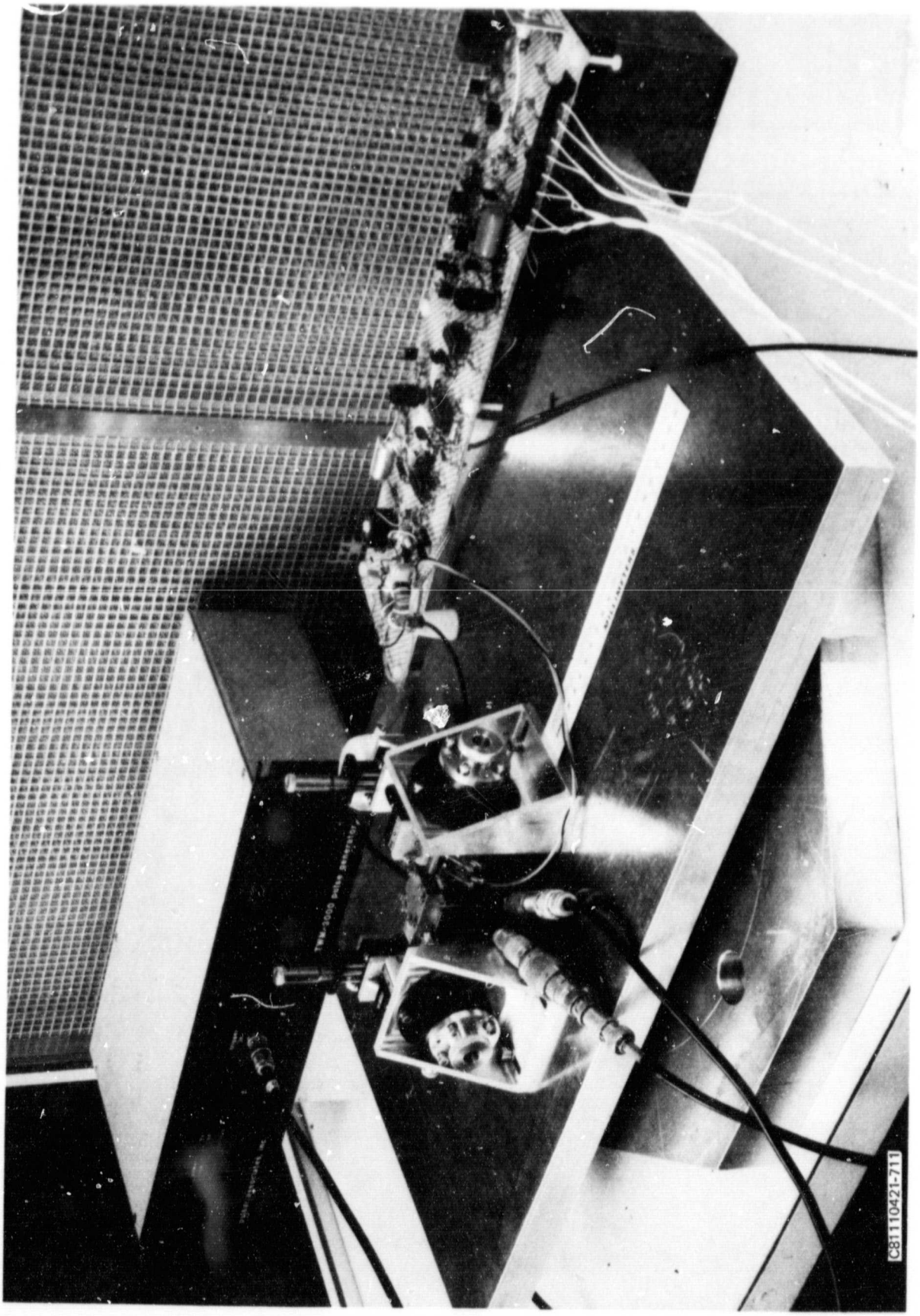

Figure 2-12. A View of the Breadboard Laser, Breadboard Electronics, and Pulsar High-Speed Driver.

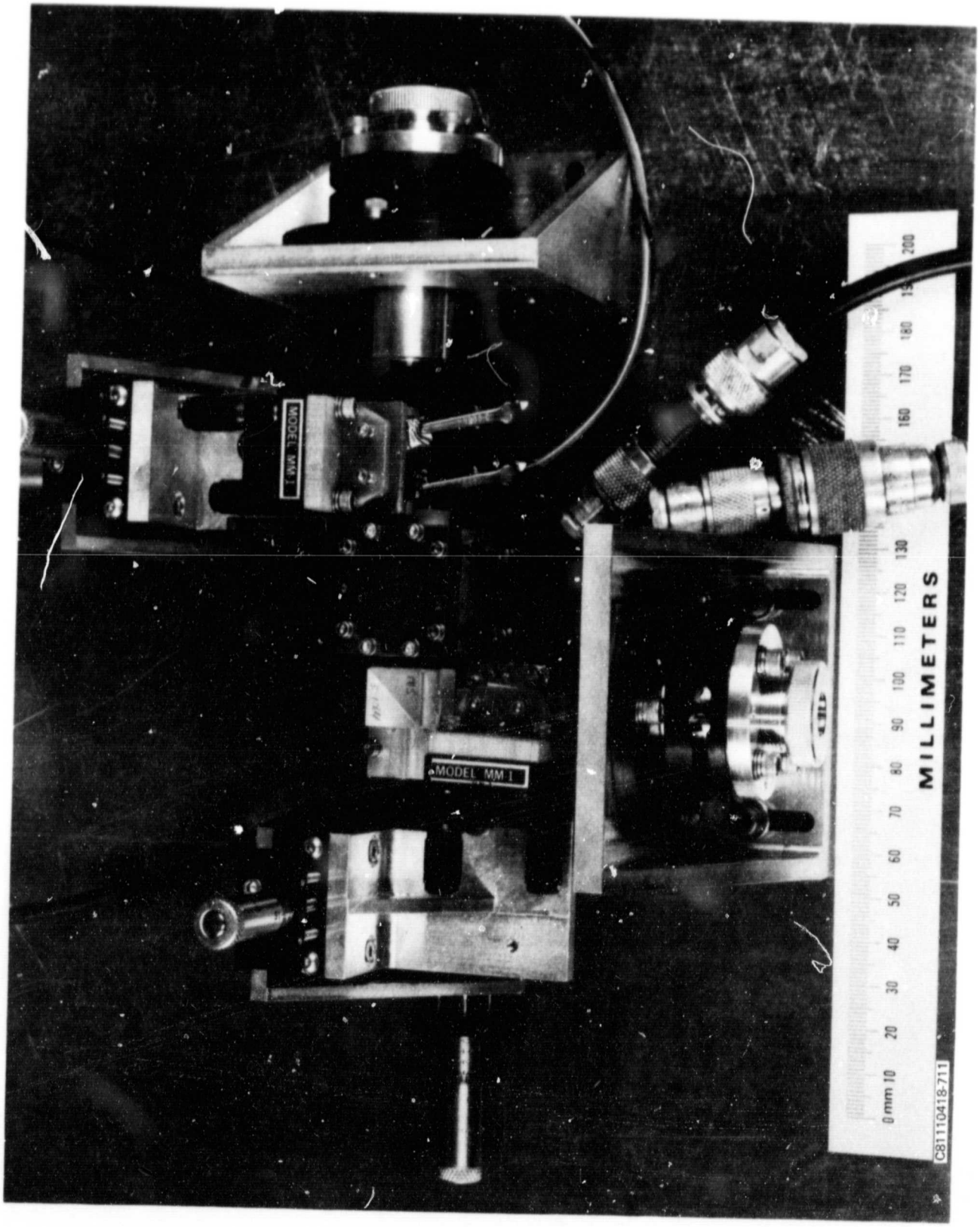

Figure 2-13. Top View of the Breadboard Laser Oscillator

Figure 2-14(a) shows the pump cavity, with the laser rod and flashlamp installed, mounted to the baseplate. The other laser components have been removed. The pump cavity is machined from copper and cooled by conduction to the baseplate (in operation, neither the pump cavity nor baseplate becomes noticeably warm.) In Figure 2-14(b) the top has been removed and inverted to show the laser rod, which is held in a shallow trough by clamps at each end. In cross section this trough has a circular shape so that it contacts the rod over the area of the trough (which corresponds to about 25 percent of the rod's cylindrical surface area). The rod is conductively cooled and gold foil is placed between the rod and trough to improve the thermal contact.

The inside of the pump cavity can also be seen in Figure 2-14(b). The cavity is cubic, 2 centimeters on a side, and is coated with Eastman white reflectance paint, a diffuse relector. The 3-millimeter bore x 2-centimeter arc-length krypton flashlamp can be seen inside the cavity. No noticeable deterioration of the Eastman paint was evident at the end of the laser testing program, after perhaps 50 hours of 10 Hz operation.

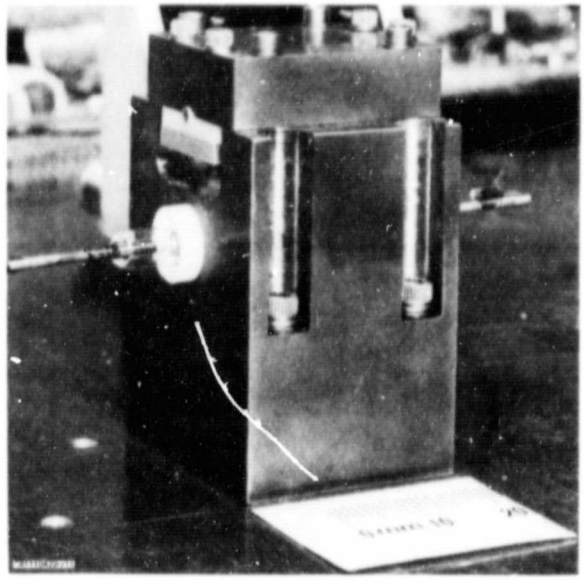

(a) Pump Cavity

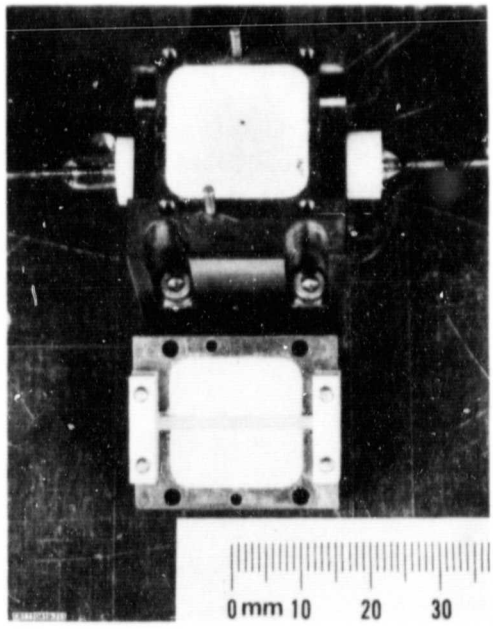

(b) Pump Cavity Opened

Figure 2-14. Conduction-Cooled Pump Cavity: (a) Assembly with Rod and Lamp; (b) Top Removed Showing the Pump Cavity and How the Rod is Mounted.

Section 3

PERFORMANCE OF THE PULSAR HIGH-SPEED DRIVER

As explained in Paragraph 2.3.1, a spark-gap switch from Pulsar, Inc. was chosen to drive the P-S crystal. This unit is packaged in a box with dimensions 3.5 x 17 x 8 inches (HxWxD). There is a BNC connector for trigger input (2 volts minimum), an RG 223/U 50-ohm cable for the output pulse, and a screwdriver adjustable potentiometer for varying the output pulse voltage amplitude. The driver was characterized in terms of output voltage, risetime, time delay between the trigger and output pulses, and output pulse time jitter.

Figure 3-1(a) shows the output voltage pulse when the cable is terminated in its characteristic impedance of 50 ohms. 70 db of (matched 50-ohm) attenuation was used between the Pulsar and the Tektronix 7104 oscilloscope to bring the approximately 2100-volt pulse to a level acceptable to the 7A29 vertical plug-in. According to the manufacturer, the risetime of this oscilloscope/plug-in combination is 380 picoseconds. From Figure 3-1(a) the measured 10 to 90 percent risetime is about 550 picoseconds. The "true" risetime t_r (true) can be estimated from

$$t_r \text{ (true)} = \sqrt{t_r^2 \text{ (measured)} - t_r^2 \text{ (instrument)}} \qquad (3\text{-}1)$$

$$t_r \text{ (true)} = \sqrt{550^2 - 380^2}$$

$$t_r \text{ (true)} = 398 \text{ picoseconds}$$

To determine how much the P-S crystal degraded this risetime, the risetime measurement was repeated with the crystal connected as shown in Figure 2-9(a). The 50-ohm load in the figure was replaced with the 7104 oscilloscope (50-ohm input impedance), and the 70 db attenuator was inserted between the crystal and the oscilloscope. The waveform shown in Figure 3-1(b) was observed, and it's risetime had degraded to about 800 picoseconds, giving an estimated "true" risetime of approximately 700 picoseconds.

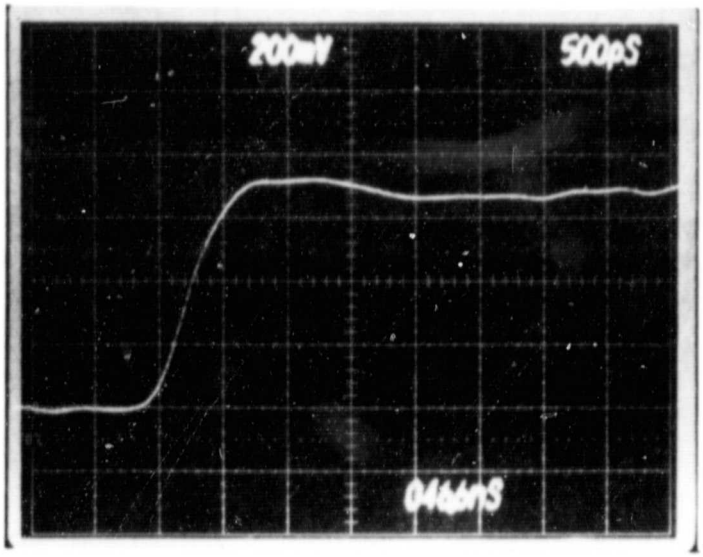

(a) 50-ohm Termination

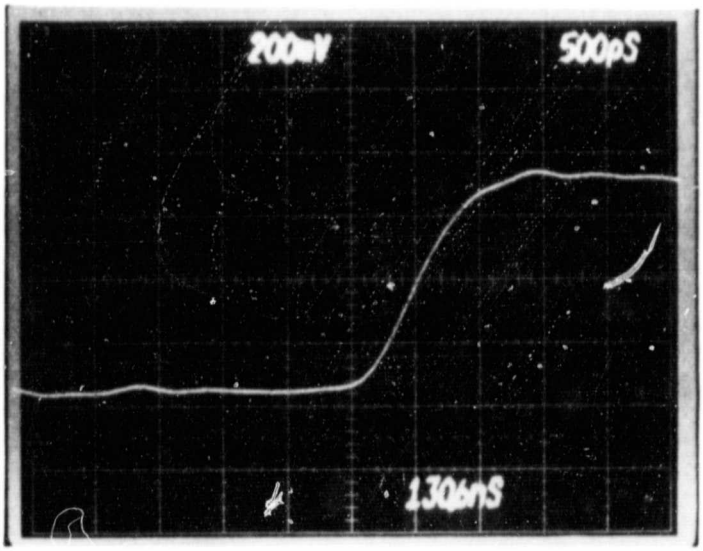

(b) Pulse-Slicer Crystal

Figure 3-1. Voltage Waveforms from the Pulsar Driver for Two Cable Termination Conditions: (a) Matched 50 ohms; (b) With $LiNbO_3$ Pulse-Slicing Crystal Driven (500 Picoseconds per Horizontal Division).

The half-power points of the optical pulse sliced from the laser resonator correspond to the 25 percent and 75 percent points on the voltage ramp of Figure 3-1(b). The "true" time interval is less than this, but is difficult to estimate.

Finally, a comment should be made concerning the observed voltage risetime and what can be inferred about the optical switching time. As discussed in Paragraph 2.3.2, the P-S crystal is connected electrically as shown in Figure 2-9(a) because its RC time constant is lower than that of the simpler configuration shown in Figure 2-9(b). Another reason for choosing (a) is that it allows the cable voltage to be monitored with the crystal in place, as was done to obtain Figure 3-1(b). At any instant, however, the cable voltage of Figure 3-1(b) is not identical to the voltage across the plates of the P-S crystal. The electric field in the crystal might not be longitudinally uniform at any instant during the switching (recall that the transit time for the electric field from one crystal end to the other is greater than 300 picoseconds), so that the "voltage across the crystal" loses its normal meaning. The optical beam responds to the effect of the integrated electrical field that it encounters while traversing the crystal. Thus, when the optical performance of the crystal is inferred from the observed cable voltage, as was done in the preceding paragraph, it has been assumed that the observed instantaneous voltage is equivalent to the instantaneous, spatially averaged voltage across the crystal. This may or may not be a good assumption.

Section 4

LASER PERFORMANCE RESULTS AND ANALYSIS

For all breadboard oscillator measurements reported in this section, the flashlamp input energy was 1.4 joules unless specified otherwise. All data were taken without using the optical gain stabilization electronics discussed in Paragraph 2.3.3. The Pulsar pulse-slicer driver was triggered a fixed time delay after the firing of the Q-switch. Most measurements were taken at a laser PRF of 10 Hz. A 20 Hz operation was verified by operating the laser continuously for 4 to 5 hours at that PRF. None of the laser performance characteristics were dependent on PRF.

4.1 THE HIGH-SPEED OPTICAL DETECTOR

The sliced optical pulses were observed using a Spectra-Physics 403B silicon detector, and the Tektronix 7104/7A29 combination discussed in Section 3. According to the manufacturers, the 403B's risetime is less than 50 picoseconds and that of the oscilloscope combination is 380 picoseconds. It is necessary to use the real-time 7104 oscilloscope for the pulsewidth measurement because the PRF of the laser is too small to permit the use of a sampling oscilloscope, which would have the advantage of a much faster risetime.

To determine the effect of the 7104's bandwidth limitation, an experiment was performed using 1064 nm output pulses from a separate laser modelocked at 150 MHz. The experiment consisted of using the 403B detector to observe the laser pulses, first with the 7104 oscilloscope, and next with a Tektronix sampling oscilloscope (7904 mainframe, 7S-11 and 7T-11 plug-ins, and S-6 sampling head). The manufacturer's risetime for the sampling setup is 30 picoseconds. Figure 4-1 shows the photographs of the oscilloscope traces. The observed pulse risetime (10 to 90 percent) with the sampling setup is about 150 picoseconds, and with the 7104 it is 300 picoseconds. The pulsewidths (FWHM) are about 300 and 470 picoseconds, respectively.

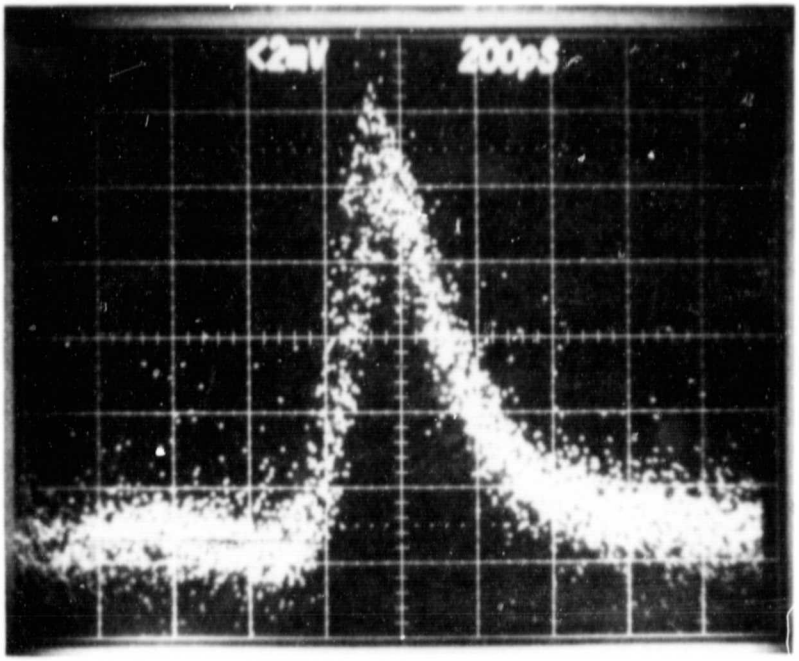

(a)

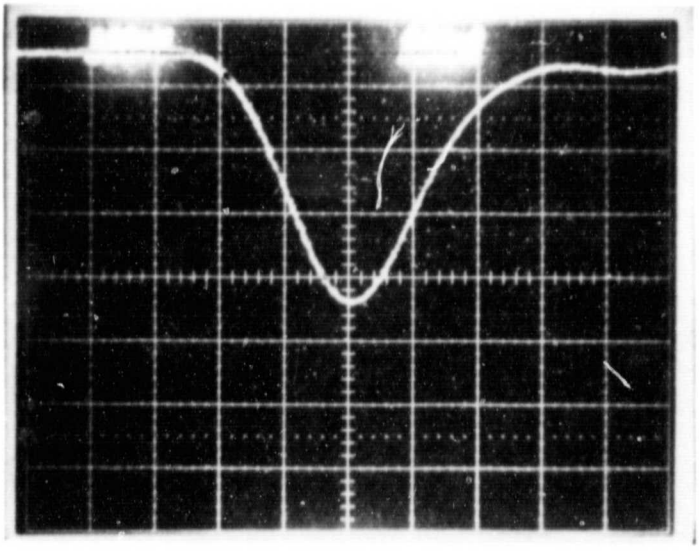

(b)

Figure 4-1. 1064-Nanometer Modelocked Laser Pulses Observed with the 403B Detector and (a) a Sampling Oscilloscope; (b) the 7104 Real-Time Oscilloscope (Pulse Inverted). Horizontal Scale was 200 Picoseconds per Division for Both Traces.

It is interesting to compute a response time τ for the 7104 oscilloscope which would degrade the "true" pulsewidth (as determined on the sampling setup) of 300 picoseconds to the measured 470 picoseconds. Using the same mathematical model used to combine risetimes,

$$(470)^2 = (300)^2 + \tau^2$$

$$\tau = 362 \text{ picoseconds} \qquad (4\text{-}1)$$

In interpreting the laser results, this response time will be used to correct the FWHM pulsewidths observed with the 7104 oscilloscope.

4.2 Q-SWITCHED OPTICAL PULSE BUILDUP AND DECAY

The intraresonator circulating power P_c was monitored by observing the leakage through the 0.5 percent transmitting mirror M_1 of Figure 2-1. Figure 4-2(a) shows this leakage when the pulse-slicer is not driven. P_c builds up and then decays due to optical losses within the resonator.

Figure 4-2(b) shows the optical pulse buildup time after Q-switch firing. A dual channel vertical oscilloscope plug-in was used and the oscilloscope was triggered from an external source. Five or six overlapping scans are shown for each trace. The upper trace shows the optical power leakage through M_1 (polarity inverted in this case), and the lower trace is the voltage on the $LiNbO_3$ Q-switch. The horizontal line is the "0" level for the lower trace. A 1000:1 voltage attenuator probe was used for the lower trace, so that the voltage scale is 500 volts/division for this case. The quarter-wave voltage for the Q-switch is about 850 volts; laser oscillation begins to occur approximately when this voltage swings through the "0" level. The buildup time is approximately 63 nanoseconds for the 1.16 joule flashlamp input used when Figure 4-2(b) was recorded. The buildup time is about 47 nanoseconds when the flashlamp input is 1.4 joules.

4.3 PULSEWIDTH OF THE PSCD OUTPUT PULSE

With the Q-switch timing and drive voltage adjusted for maximum optical circulating power, the timing (relative to the firing of the Q-switch) and drive voltage of the Pulsar pulse-slicer driver were adjusted to optimize the PSCD optical output

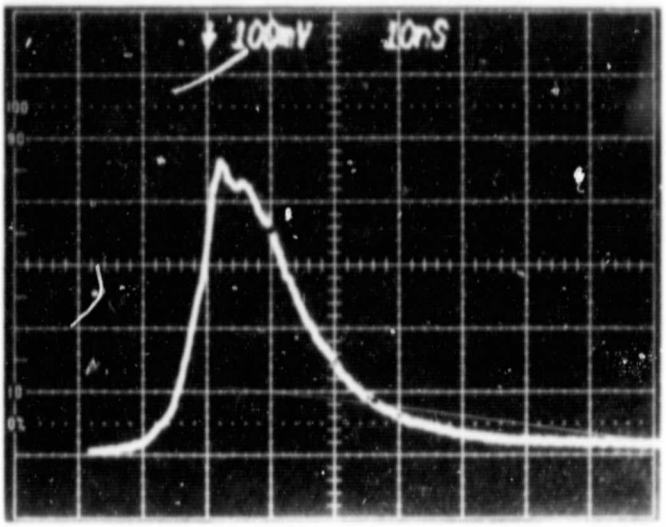

(a) 10 Nanoseconds per Horizontal Division

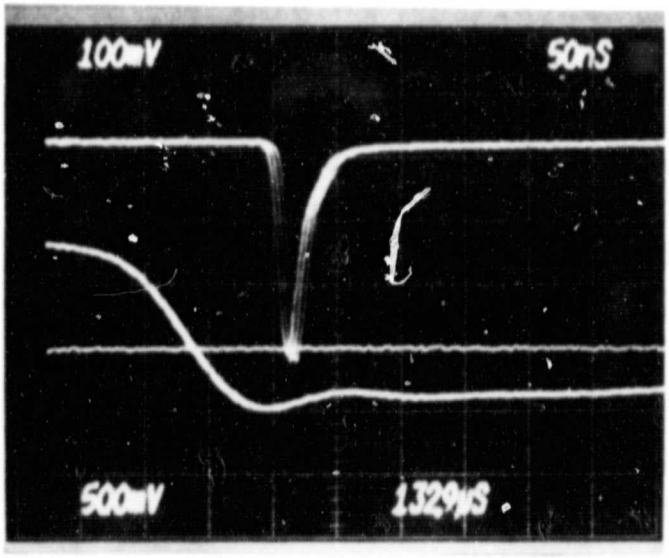

(b) 50 Nanoseconds Per Horizontal Division

Figure 4-2. Intraresonator Q-switched Pulse and its Buildup Time (Pulse-slicer was not operated). Lower trace in (b) shows the Q-switch voltage on a vertical scale of 500 volts per division.

pulse (minimum pulsewidth, best shape). Figure 4-3 shows the optical output pulse, as detected using the Spectra-Physics 403B photodiode and the Tektronix 7104 oscilloscope. In (a), the observed FWHM pulsewidth is 560 picoseconds. Using equation (4-1), the estimated "true" pulsewidth is 427 picoseconds.

Noticeable in both (a) and (b) of Figure 4-3 is the leakage of optical energy after the pulse-slicer has been switched. This would be expected if the voltage pulse to the slicer were too small in amplitude, but it was adjusted to minimize this leakage. The cause is probably electro-optical in origin, since mechanical strains would not be expected to develop in the very short time scale shown.

4.4 PULSE OUTPUT ENERGY

The energy content of the output pulse was measured using an Eppley thermopile and a digital microvoltmeter. The sensitivity of the thermopile is 5.63 watts per volt. Measuring the average power and dividing by the PRF gave a measured pulse energy of 416 microjoules. However, as shown in Figure 4-3, not all of this energy is contained within the narrow, sliced pulse. In fact, based on estimates from Figure 4-3 and other similar photographs (not shown), as much as 45 to 50 percent of the measured pulse energy might be contained within the low-level leakage. The energy content of the main, sliced pulse is therefore estimated to be 225 ± 75 microjoules.

4.5 JITTER

The amplitude of the pulse-sliced optical output was observed to jitter by about ±15 percent over time periods of 1 minute. There are two reasons for this: fluctuations in the flashlamp input energy, and time jitter associated with the Pulsar triggering. Fluctuations in the flashlamp energy lead to pulse-to-pulse variations in the peak value of the intraresonator circulating power, and also cause variations in the buildup time. These effects are noticeable in Figure 4-2(b).

Measurements on the Pulsar showed that there was a delay of about 150 nanoseconds between the time that the trigger signal was applied to it and the appearance of the high-voltage output pulse. Furthermore, there was a short-term (over time periods of a few seconds) jitter of about ±3 nanoseconds associated with this delay. This can be seen in Figure 4-4, which shows 15 to 20 high-voltage pulses. The oscilloscope's horizontal sweep was triggered by the trigger-input pulse to the Pulsar.

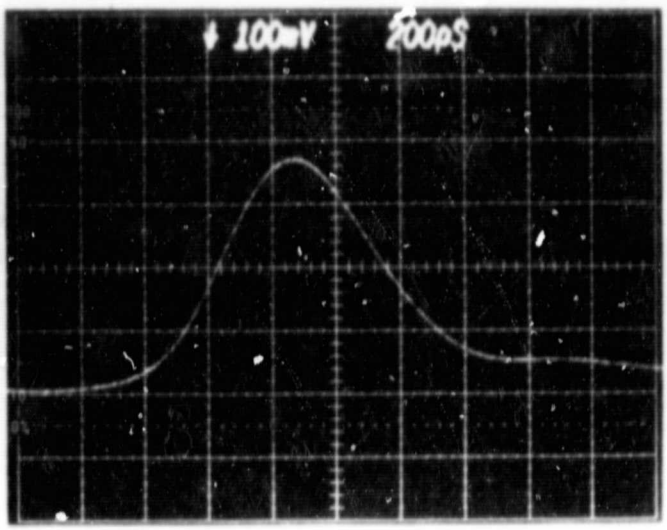

(a) 200 Picoseconds per Horizontal Division

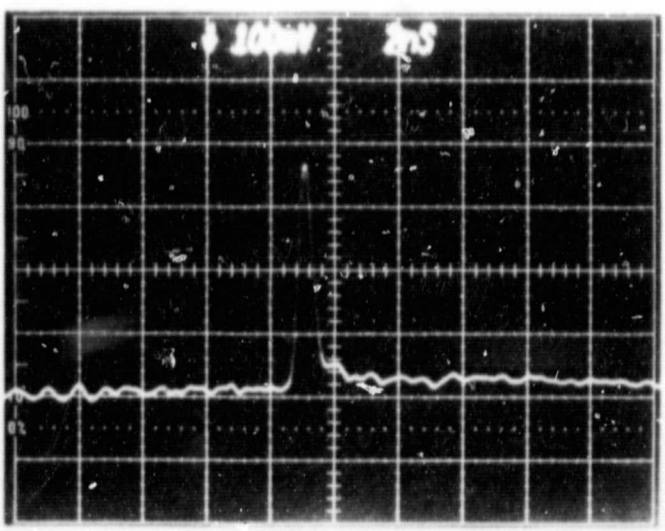

(b) 2 Nanoseconds per Horizontal Division

Figure 4-3. Pulse-Sliced Optical Output

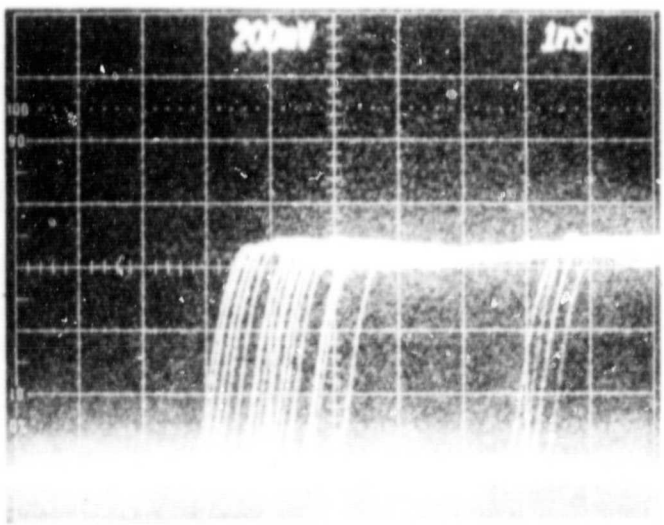

Figure 4-4. Time Jitter in the High-Voltage Pulse from the Pulsar Unit. (The oscilloscope was triggered by the trigger input signal to the Pulsar. Horizontal scale was 1 nanosecond per division.)

4.6 MEASURED OPTICAL CIRCULATING POWER DENSITY

The intraresonator optical circulating energy was monitored by measuring the power leakage through the 0.50 percent-transmitting mirror M_1 (Figure 2-1). With the pulse-slicer not operating, it was measured to be 13.2 millijoules per pulse. Using the measured FWHM pulsewidth of 17 nanoseconds shown in Figure 4-2(a), this corresponds to a peak power of 0.78 megawatts (MW).

The oscillating beam does not completely fill the 2-millimeter diameter rod. Using apertures in front of the thermopile, it was found that 90 percent of the beam energy is contained within a beam of diameter 1.7 millimeters. Using this for the beam size, the peak circulating power density inside the resonator was computed to be 34.4 MW/cm^2.

4.7 BEAM DIVERGENCE

The beam divergence of the pulse-sliced optical output was determined by measuring the beam size on a screen several meters from the laser. It was observed that most (> 85 percent) of the beam energy was contained within a divergence angle of about 6.5 milliradians. This was independent of laser PRF from 1 to 20 Hz. The theoretical divergence was predicted using Equations (2-1) through (2-3). The resonator b parameter is given by

$$b = \sum_{i=1}^{n} \frac{\ell_i}{n_i} \quad , \tag{4-1}$$

where ℓ_i is the length of a resonator element and n_i is its refractive index (air spaces are also included, for which n=1). The value b was measured to be 8.8 centimeters for the breadboard oscillator. Theoretically, the value of the rod thermal focusing is expected to be negligible; this is supported by the observation that the output beam divergence is independent of laser PRF. Using a beam diameter D of 1.7 millimeters in Equation (2-1) results in a value of 7.9 milliradians for the predicted full-angle beam divergence. This compares favorably with the observed value of 6.5 milliradians.

4.8 ANALYSIS

It is interesting to compare the results of the laser energy measurements with the predictions of theory. Table 4-1 summarizes the relevant measurement results.

Table 4-1. Some Measured Operating Characteristics of the Breadboard Oscillator

1. Q-switched optical pulse decay time	11.5 ns
2. P_c (max)	.78 MW
3. P_c/A (max)	34.4 MW/cm^2
4. N_m/N_t (1.4 J lamp input)	~2.3
5. Resonator optical transit time (round trip)	1.37 ns
6. PSCD pulse energy	225 ± 75 μJ

The Q-switched optical pulse decay time was determined from Figure 4-2(a); the trailing edge of this Q-switched pulse fits closely the relationship

$$I = I_0 \, e^{-t/11.5 \text{ ns}} \quad . \tag{4-2}$$

This can be used to estimate the single-pass optical loss Λ of the resonator because the decaying intensity should follow

$$I_0 \, e^{-2t(\Lambda - g_r)/1.37 \text{ ns}} \tag{4-3}$$

where g_r is the residual single-pass optical gain coefficient after Q-switching. For operation at 2.3 times threshold, g_r is approximately 0.3Λ[5]. Comparing Equations (4-2) and (4-3) yields a value for Λ of 0.09.

At 1.4 joules flashlamp input energy the laser was operating at about 2.3 times the threshold value of the flashlamp input energy, as reported in Table 4-1. This was determined by reducing the flashlamp input until the laser ceased to operate. Knowing this, the experimental results can be compared to the theoretical predictions, which have been summarized in Figure 2-2. The figure shows that when the oscillator is pumped at approximately 2.3 times its threshold level, a peak circulating power density of about 30 MW/cm^2 should be achieved when the single-pass optical loss is just below 10 percent. This is in excellent agreement with the measured value of 34.4 MW/cm^2.

Finally, the PSCD pulsewidth can be estimated from the measured value of P_c(max) and the estimated energy content of the pulse. These yield a pulsewidth of 225 μJ/.78 MW = 288 picoseconds. Because of the uncertainty in the measured value of the pulse energy (225 ±75 μJ), this calculated pulse width is not inconsistent with the measured value of 425 ±50 picoseconds.

Section 5

CONCLUSIONS AND RECOMMENDATIONS

The Mini-Cavity-Dumped Laser program consisted of two parallel efforts: the development of a miniature Q-switched laser oscillator and the development of a high-speed, high-voltage driver for the optical pulse-slicing crystal. Table 1-1 summarizes the breadboard oscillator's performance.

The high-speed driver, designed and fabricated by Pulsar, Inc., performs well. It has an adjustable voltage output of approximately 2 to 3 kilovolts, and a 10 to 90 percent risetime of about 400 picoseconds when terminated in its characteristic impedance of 50 ohms. When loaded with the P-S crystal, however, the risetime degrades to approximately 700 picoseconds, somewhat longer than the goal of 500 picoseconds. The degraded risetime is probably due largely to the crystal capacitance of 9 picofarads, which is substantially greater than the 6 picofarad value used in the design phase of the program (the crystal's size was modified during the laser testing phase). The switching speed could undoubtedly be increased by impedance matching the driver cable (50 ohms) to the characteristic impedance of the crystal (6 ohms). This could not be accomplished on the program because it requires a voltage of about 6 kilovolts from the driver, double the capability of the Pulsar unit.

The Q-switched oscillator was operated at an intraresonator optical power density of about 34 MW/cm^2, just under the damage threshold of $LiNbO_3$. The laser was pumped at approximately 2.3 times threshold, with a measured single-pass optical loss of 9 percent. This is in good agreement with the theory which was worked out for the oscillator.

The PSCD optical pulse was measured using a detector and real-time oscilloscope whose combined risetime, according to the manufacturers, is 380 picoseconds. The PSCD pulsewidth, after correction for the instrument response time, is estimated to be 425 ± 50 picoseconds. The method used to correct the observed pulsewidth (560 picoseconds) is not rigorous, resulting in the error estimate of ±50 picoseconds.

The Mini-Cavity-Dumped Laser program showed the feasibility of using pulse-slice cavity dumping (PSCD) to achieve very short optical pulsewidths. Future work on the oscillator should be concentrated in two areas. First, its mechanical design should be improved, because little effort was expended in this area of the program. The optics mounts, pump cavity, and cooling system (if any) should be designed to be compatible with the eventual mobile satellite ranging system and its environment. Second, the switching speed of the PSCD driver and crystal combination should be increased to achieve pulsewidths the order of 250 to 300 picoseconds. Possibly the pulsewidths can be achieved by decreasing the 3-millimeter width of the pulse-slicer crystal to 2 millimeters. This would reduce its capacitance and the optical pulsewidth could approach 300 picoseconds. Even shorter optical pulses could be achieved by redesigning the Pulsar to provide twice its present voltage amplitude, and impedance matching it to the pulse-slicer crystal.

REFERENCES

1. R. H. Dishington, "Energy Extraction Optimization in Lasers," SPIE Vol.69, 135, (975).

2. A. W. Warner et al., "Determination of Elastic and Piezoelectric Constants for Crystals in Class (3m)," Journal of the Acoutical Society of America, 42, 1223 (Dec. 1967).

3. D. C. Downs et al., "Stabilizing the Output of a Q-Switched Laser," Journal of Quantum Electronics, QE-14, 571 (August 1978).

4. J. P. Markiewicz and J. L. Emmett, "Design of Flashlamp Driving Circuits," Journal of Quantum Electronics, QE-2, 707, (November 1966).

5. Walter Koechner, "Solid State Laser Engineering," Springer-Verlag, 1976. Page 401.